eLIFE elifesciences.org

RESEARCH ARTICLE

Figures and figure supplements

The fail-safe mechanism of post-transcriptional silencing of unspliced *HAC1* mRNA

Rachael Di Santo *et al*

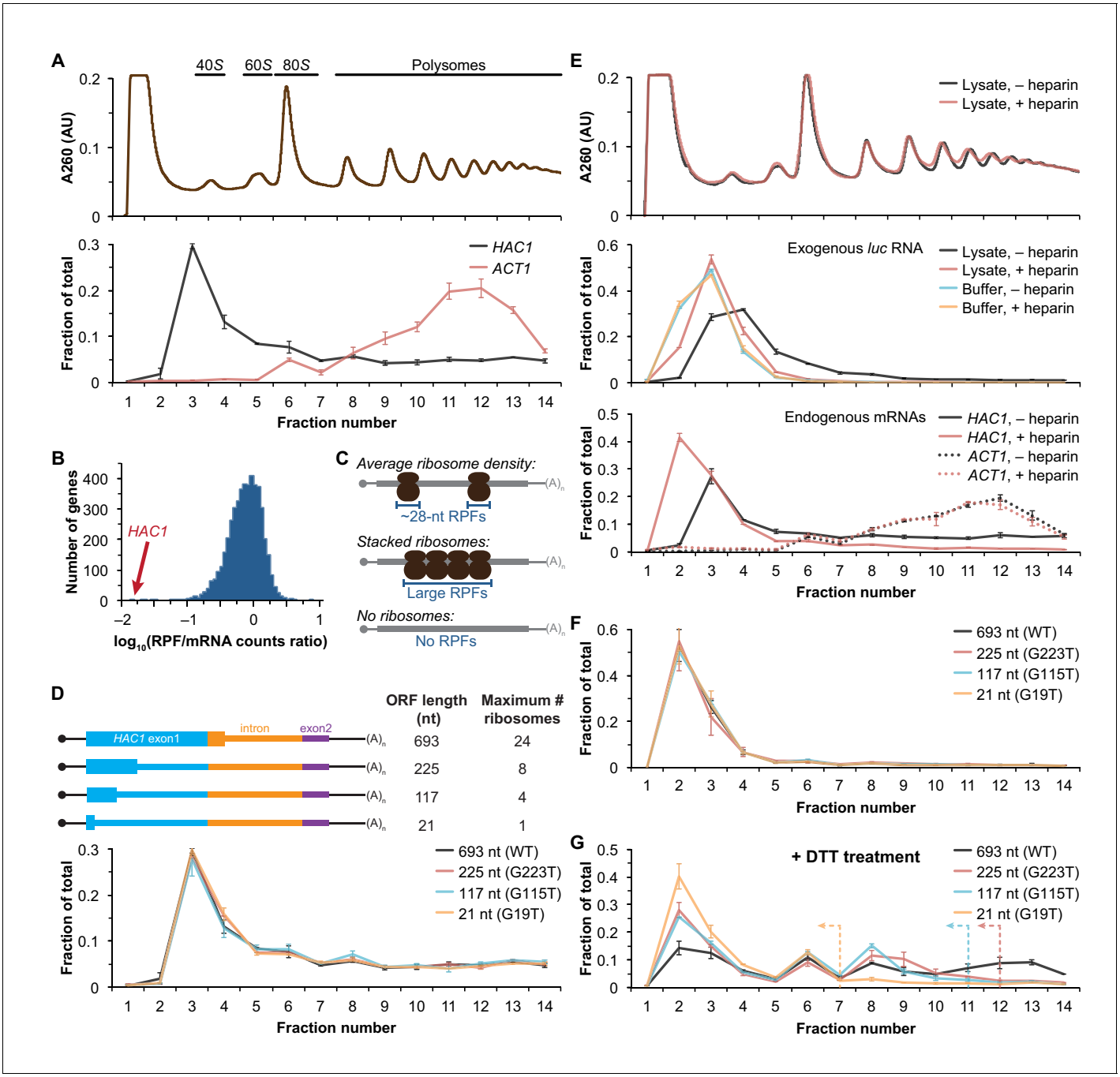

Figure 1. Ribosome density on unspliced *HAC1* mRNA. (**A**) Polysome analysis of *HAC1* and *ACT1* mRNAs. Extracts prepared from exponentially growing yeast cells were fractionated on 10–50% sucrose gradients, with absorbance at 260 nm monitored (top). The relative distributions of *HAC1* and *ACT1* mRNAs across fractions were determined by qRT-PCR (bottom). Shown are the mean ± SEM with $n = 2$ (i.e., the range), expressed as a fraction of the total mRNA detected. (**B**) Histogram of ribosome densities measured by ribosome profiling and RNA-seq. The ratio of the number of ribosome-protected fragments (RPFs) to the number of RNA-seq reads (mRNA counts) was calculated for each of 4838 expressed yeast genes (data from ***Weinberg et al., 2016***). Shown is the distribution of log-transformed ratios in bins of 0.05, with the position of *HAC1* indicated. (**C**) Possible scenarios to explain a lack of RPFs. While an mRNA with average ribosome density will generate many ~28 nucleotide (nt) RPFs (top), the close packing of stacked ribosomes could inhibit the RNase digestion between ribosomes required to generate ~28 nt RPFs (middle). Alternatively, an mRNA that does not contain translating ribosomes would not generate RPFs (bottom). (**D**) Polysome analysis of *HAC1* mRNA variants with shortened ORFs. G-to-T point mutations were introduced into the first exon of *HAC1* to generate premature stop codons, with the resulting ORFs shown as thick colored boxes (constitutive 5′- and 3′-UTRs located within exons 1 and 2, respectively, are shown as thin black lines; other untranslated regions are depicted as thin colored boxes; and the coding regions of exons 1 (teal) and 2 (purple) are labeled as '*HAC1* exon1' and 'exon2', respectively). The maximum number of

Figure 1 continued on next page

Figure 1 continued

ribosomes that could be accommodated was calculated based on each ribosome occupying 28 nt. Polysome analysis was performed as in (**A**), with data for wild-type *HAC1* from (**A**) duplicated for comparison. (**E**) Effects of heparin on polysome analysis. Purified uncapped *luciferase* (*luc*) RNA was added to either lysate or lysis buffer in the absence (–) or presence (+) of 0.2 mg/ml heparin. Polysome analysis was performed as in (**A**) with absorbance at 260 nm monitored (top), and the relative distributions of exogenous *luc* RNA (middle) and endogenous *HAC1* and *ACT1* mRNAs (bottom; in lysate only) were determined. (**F**) Refined polysome analysis of *HAC1* mRNAs. Extracts were prepared in heparin-containing lysis buffer from strains shown in (**D**). Polysome analysis was performed as in (**A**). (**G**) Polysome analysis of *HAC1* mRNAs during the UPR. Strains shown in (**D**) were grown to mid-log phase and treated with 8 mM DTT for 20 min before harvesting. Extracts were prepared in heparin-containing lysis buffer, and polysome analysis was performed as in (**A**). Dotted lines indicate the fractions after which the corresponding color-coded mutant mRNAs would not be expected to sediment based on ORF length.

DOI: 10.7554/eLife.20069.003

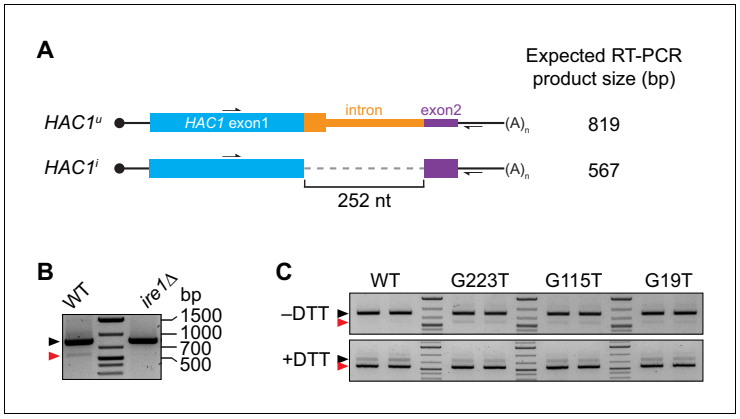

Figure 1—figure supplement 1. Splicing of *HAC1* mRNA. (**A**) Design of RT-PCR assay for *HAC1* splicing. To differentiate between the *HAC1*^{u} and *HAC1*^{i} mRNAs, reverse-transcription products are PCR amplified using a pair of primers that flank the intron. The resulting PCR products are separated by agarose gel electrophoresis, with a size difference of 252 base pairs (bp) corresponding to the size of the intron. (**B**) Splicing status of *HAC1* mRNA. Total RNA was extracted from exponentially growing yeast cells of the indicated genotypes. RT-PCR across the intron was used to differentiate between unspliced (black arrow) and spliced (red arrow) *HAC1* mRNA. The small percentage of spliced *HAC1* mRNA observed in wild-type cells is *IRE1* dependent, as expected. (**C**) Splicing of *HAC1* mRNA variants upon DTT treatment. Strains expressing the indicated *HAC1* variants were grown to mid-log phase and either left untreated (–DTT) or treated with 8 mM DTT for 20 min (+DTT) before harvesting. Total RNA was extracted and used for RT-PCR analysis as in (**A**). The same cultures (two of each strain) were used for polysome analysis in ***Figure 1F and G***.

DOI: 10.7554/eLife.20069.004

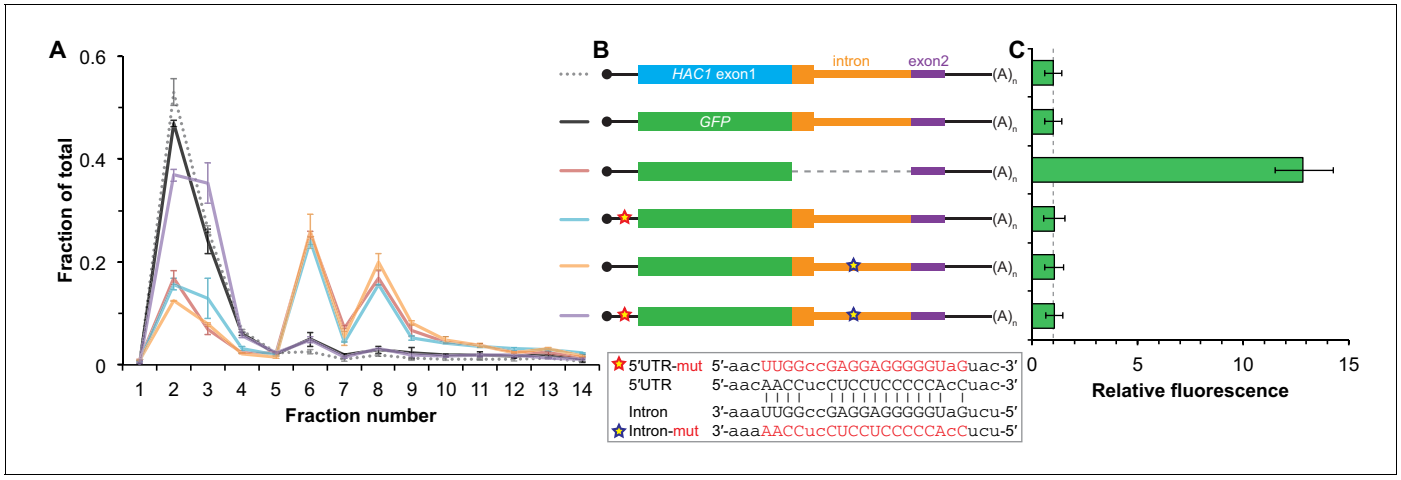

Figure 2. Contribution of long-range base pairing to intron-dependent silencing. (**A**) Polysome analysis of reporter mRNAs. Extracts were prepared in heparin-containing lysis buffer from strains expressing the *GFP* reporter mRNAs depicted in (**B**). Polysome analysis was performed as in ***Figure 1A***, with data for wild-type *HAC1* from ***Figure 1F*** duplicated for comparison. (**B**) Design of reporter mRNAs. Constructs are depicted as in ***Figure 1D***, with the dotted line indicating a deleted region. Colored stars indicate mutations to the base-pairing region, with specific nucleotide changes shown below in red. (**C**) Flow cytometry analysis of reporter strains. Strains expressing the *GFP* reporter mRNAs depicted in (**B**) were grown to mid-log phase and analyzed by flow cytometry. Plotted is the median GFP intensity (normalized to cell size) of the cell population relative to background fluorescence in the wild-type (no GFP) strain with error bars indicating quartiles of the cell population, all averaged across replicates (n = 2–7).

DOI: 10.7554/eLife.20069.005

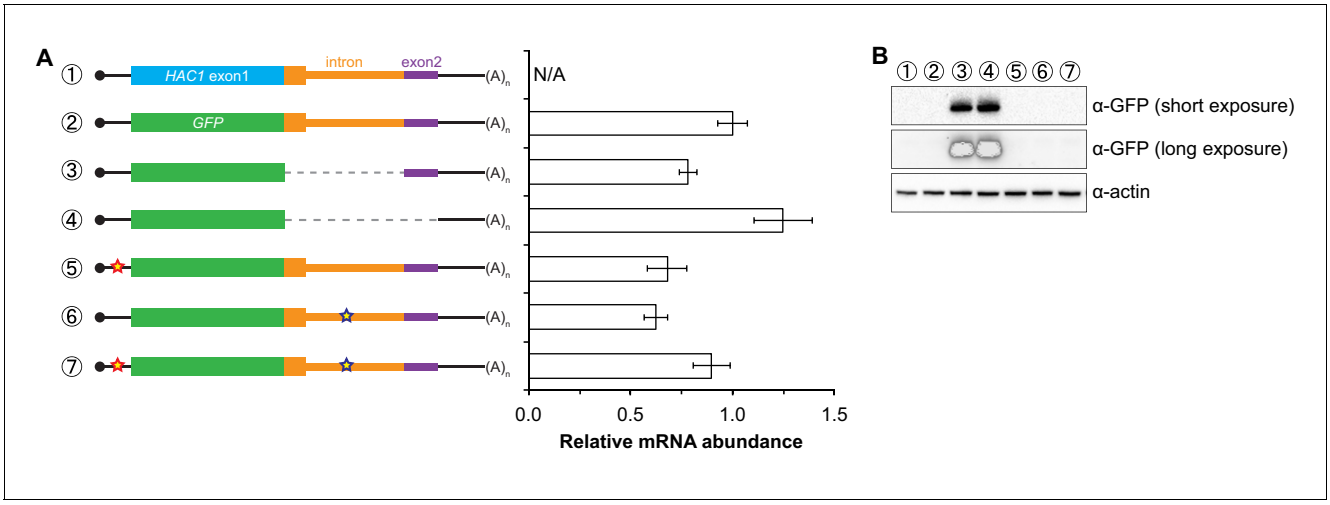

Figure 2—figure supplement 1. Characterization of *GFP* reporter strains. (**A**) RNA abundance measurements for *GFP* reporter mRNAs. Total RNA was extracted from strains expressing the indicated mRNAs, using the same cultures as for flow cytometry analyses in ***Figure 2C***. qRT-PCR was used to measure the abundances of *GFP* reporter mRNAs relative to *ACT1* mRNA, with all data normalized to the abundance of the 'wild-type' *GFP* reporter mRNA (construct 2). Shown are the mean ± SD (*n* = 2–7). (**B**) Immunoblotting analysis of reporter strains. Proteins were extracted from mid-log-phase cultures of strains expressing the indicated reporter mRNAs depicted in (**A**). Immunoblots for the GFP reporter and actin loading control are shown. No signal for GFP is observed in the base-pairing mutants (constructs 5 and 6) even after overexposing the blot, consistent with the corresponding flow cytometry results (***Figure 2C***).

DOI: 10.7554/eLife.20069.006

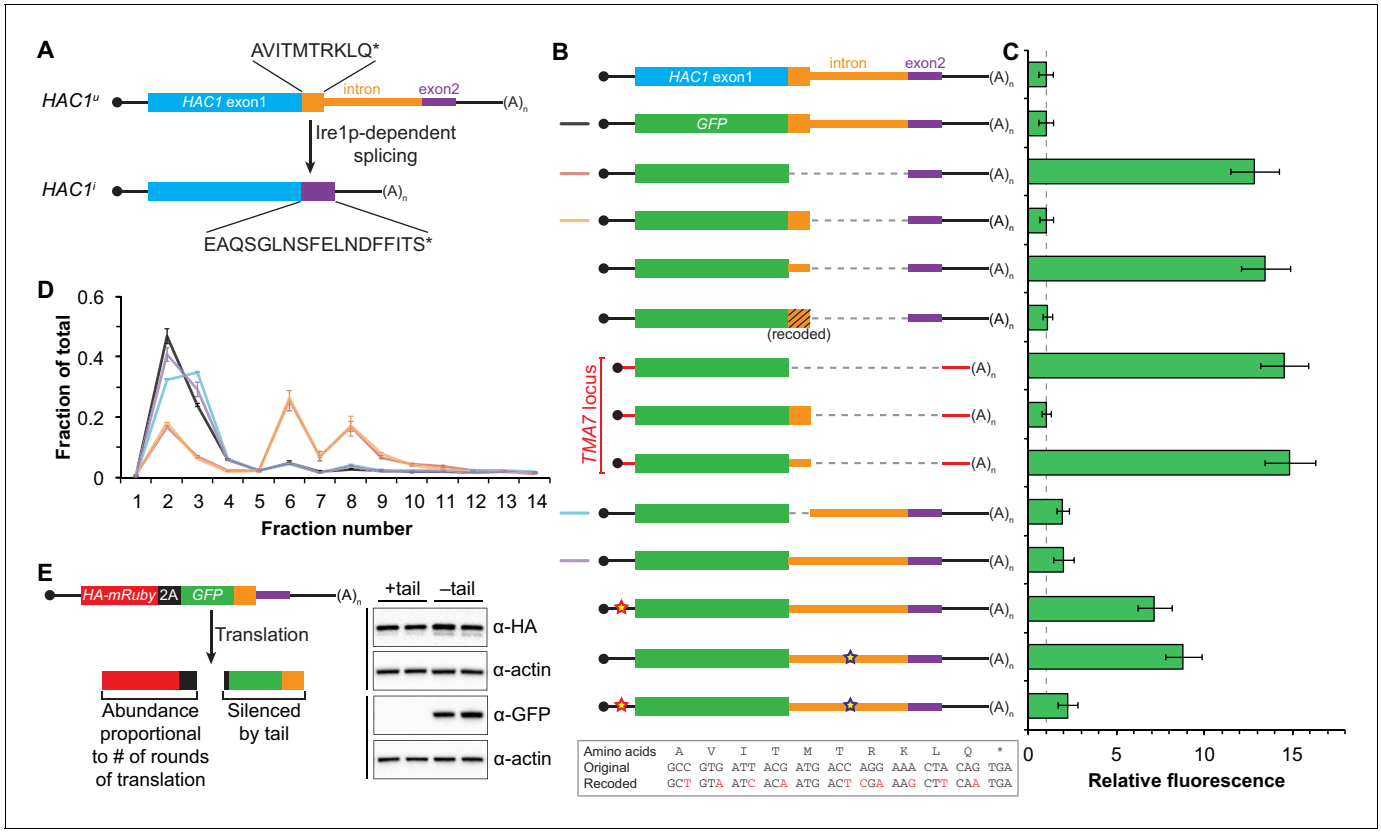

Figure 3. Post-translational silencing mediated by the intron-encoded C-terminal tail. (**A**) Schematic of *HAC1* mRNA splicing. The proteins encoded by *HAC1*^{u} and *HAC1*^{i} mRNAs differ in their C-terminal tails, with the amino acid sequences indicated. (**B**) Design of reporter mRNAs. Black shading indicates recoding, with the original and recoded sequences depicted below (mutations in red). Untranslated regions colored red correspond to those of the *TMA7* mRNA, with the reporter gene integrated at the *TMA7* rather than *HAC1* locus. Otherwise constructs are depicted as in ***Figure 2B***. (**C**) Flow cytometry analysis of reporter strains. Strains expressing the *GFP* reporter mRNAs depicted in (**B**) were analyzed as in ***Figure 2C***, with data for the first three strains duplicated from ***Figure 2B*** for comparison. (**D**) Polysome analysis of reporter mRNAs. Extracts were prepared in heparin-containing lysis buffer from strains expressing the *GFP* reporter mRNAs indicated in (**B**). Polysome analysis was performed as in ***Figure 1A***, with data for the wild-type and intronless *GFP* reporters from ***Figure 2A*** duplicated for comparison. (**E**) Differentiating between co-translational and post-translational silencing mechanisms. Left: Schematic of reporter construct that generates two separate polypeptides from each round of translation. Right: Extracts were prepared from strains expressing reporter mRNAs that either encoded the 10-amino-acid C-terminal tail of Hac1^{u}p (+tail) or contained a stop codon just before the tail (–tail). Immunoblotting was used to detect HA-tagged mRuby (top) and GFP (bottom), with actin as a loading control. Two biological replicates are shown for each genotype.

DOI: 10.7554/eLife.20069.007

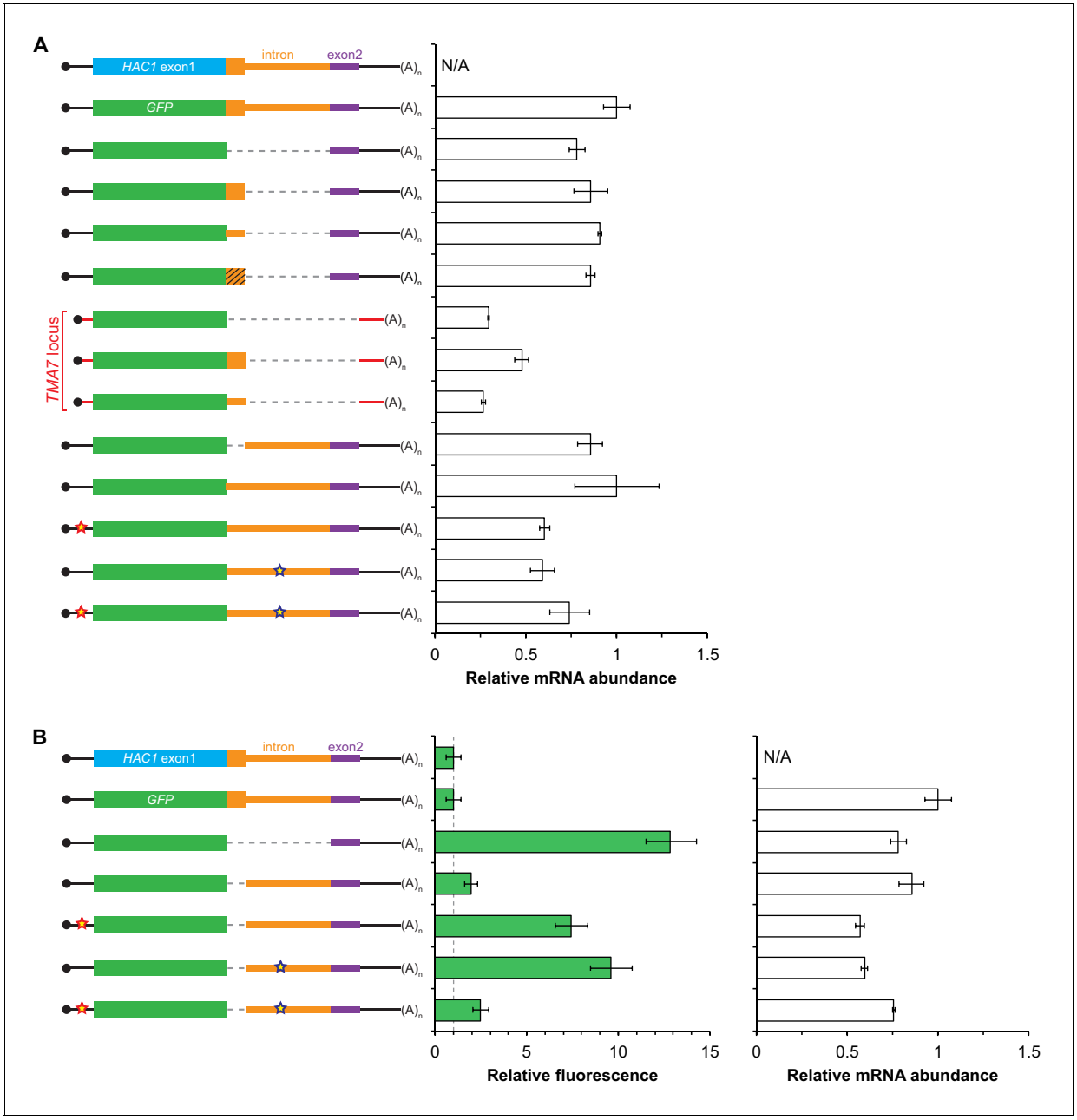

Figure 3—figure supplement 1. Additional analyses of *GFP* reporter constructs. (**A**) RNA abundance measurements for *GFP* reporter mRNAs, analyzed as in ***Figure 2—figure supplement 1A*** using the same cultures as for flow cytometry analyses in ***Figure 3C***. (**B**) Flow cytometry and RNA analyses of additional reporter strains. Strains expressing the indicated *GFP* reporter mRNAs (left) were analyzed by flow cytometry as in ***Figure 2C*** (middle) or qRT-PCR as in ***Figure 2—figure supplement 1A*** (right), with data for the first four strains duplicated from ***Figure 3C*** and ***Figure 3—figure supplement 1A*** for comparison.

DOI: 10.7554/eLife.20069.008

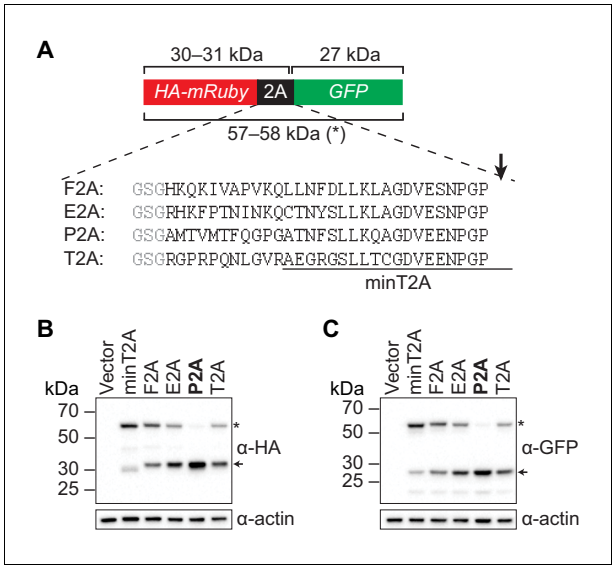

Figure 3—figure supplement 2. Identifying a 2A peptide sequence that is active in *S. cerevisiae*. (**A**) Design of the 2A reporter construct. In the absence of 2A activity, a 57–58 kDa polypeptide (*) is produced that contains both an HA tag and GFP. When the 2A sequence is active, translation of the reporter generates a 30–31 kDa HA-tagged protein and a 27 kDa GFP. Shown are the 30-amino-acid sequences of the 2A peptides that were tested, with each preceded by a GlySerGly linker (gray) and 'cleaved' at the site marked with an arrow. The region corresponding to a minimal 20-amino-acid T2A peptide ('minT2A') that has been used previously in yeast (***Beekwilder et al., 2014***) is indicated. Minimal versions of the F2A peptide have also been used in yeast (***Doronina et al., 2008***; ***de Felipe et al., 2003***; ***Sharma et al., 2012***; ***Voordeckers et al., 2012***) but with 'cleavage' efficiencies that were low or not directly measured. (**B–C**) Analysis of 2A activity by immunoblotting. BY4741 was transformed with a pRS413-derived centromeric plasmid containing the indicated reporter construct under control of the *GPD* promoter. Proteins were extracted from mid-log-phase cultures and analyzed for HA- (**B**) and GFP- (**C**) tagged proteins by immunoblotting. Only the P2A peptide causes efficient separation of the upstream and downstream proteins (indicated by arrows). The nucleotide sequences encoding the 30-amino-acid peptides are:

F2A: CACAAACAAAAGATTGTTGCGCCTGTGAAACAGCTTTTGAACTTTGACCTGCTCAAG TTGGCAGGAGACGTCGAGTCCAACCCTGGGCCT

E2A: AGACATAAATTTCCCACTAACATCAACAAACAGTGTACTAATTACTCTCTCCTCAAATTGGCTGGAGATG TTGAGAGCAACCCTGGC CCC

P2A: GCTATGACTGTGATGACATTCCAGGGACCAGGTGCAACAAACTTCTCCCTCTTGAAACAAGCAGGAGA TGTTGAGGAAAATCCCGGGCCT

T2A: CGGGGGCCTCGCCCCCAAAACCTTGGGGTAAGGGCCGAGGGCAGGGGAAGTCTTCTAACA TGCGGGGACGTGGAGGAAAATCCCGGCCCC

DOI: 10.7554/eLife.20069.009

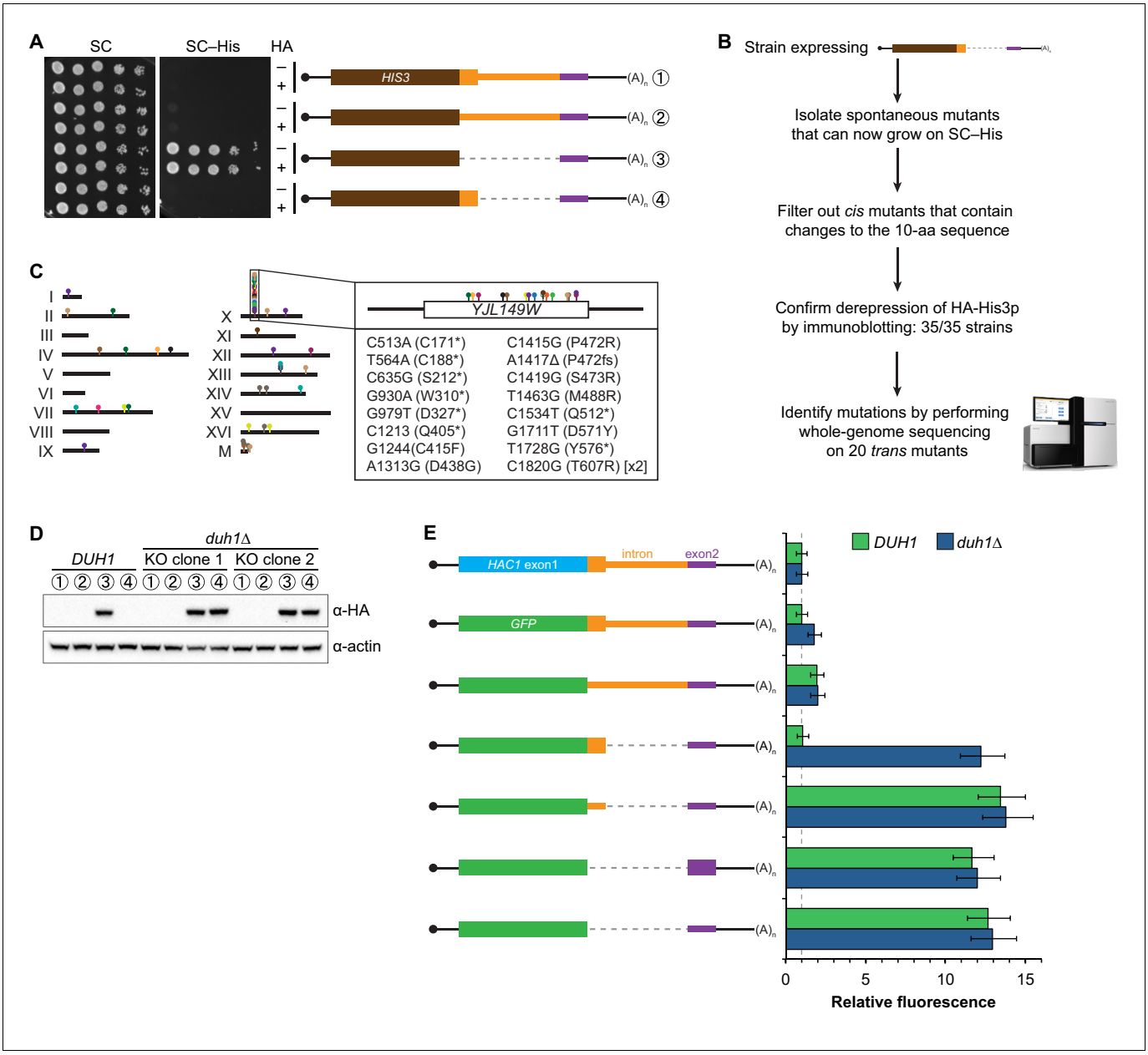

Figure 4. Identification of *DUH1* through a genetic selection. (**A**) Evaluating a genetic reporter for intron-dependent silencing. Strains expressing the indicated *HAC1*-based *HIS3* reporter mRNAs (depicted as in ***Figure 2B***) either without (–) or with (+) an N-terminal HA tag were grown to saturation, and 10-fold dilution series were plated on either SC or SC–His media. (**B**) Flowchart of genetic selection for *dds* mutants. After selecting for spontaneous mutants that could grow on medium lacking histidine, restreaked clones were filtered out for *cis* mutants, verified to be expressing HA-His3p, and a subset analyzed by whole-genome sequencing. (**C**) Chromosome map of mutations identified by whole-genome sequencing. Each color corresponds to a different *dds* mutant strain. Shown on the right is the *DUH1* locus (*YJL149W*), with locations of nucleotide changes (with respect to *DUH1* start codon) and corresponding amino changes listed below. (**D**) Effect of *DUH1* disruption on expression of the genetic reporter. Strains expressing the indicated reporter mRNAs depicted in (**A**) in either a *DUH1* or *duh1Δ* (two independent clones) background were grown to mid-log phase. Extracts were prepared and immunoblotted for HA-His3p and actin loading control. (**E**) Flow cytometry analysis of reporter strains. Strains expressing the indicated *GFP* reporter mRNAs in either a *DUH1* or *duh1Δ* background were analyzed as in ***Figure 2C***. Data is plotted as in ***Figure 2C*** (*n* = 2 for all strains).

DOI: 10.7554/eLife.20069.010

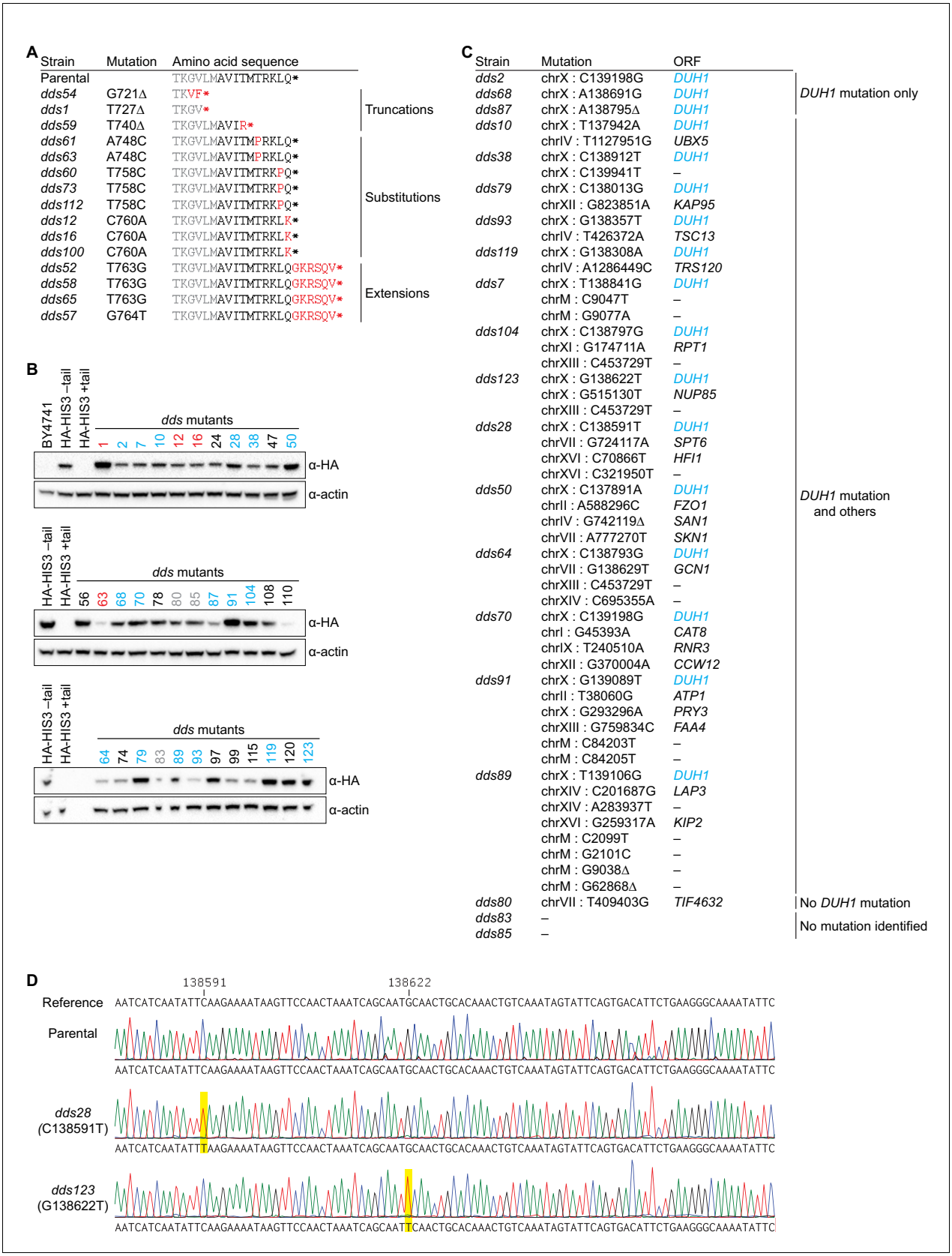

Figure 4—figure supplement 1. Results and validation of the genetic selection. (**A**) Table of *cis*-acting mutations identified by Sanger sequencing. In the parental strain, the Hisp3-coding sequence is shown in gray while the 10-amino-acid degron is shown in black. Amino-acid changes caused by

Figure 4—figure supplement 1 continued on next page

Figure 4—figure supplement 1 continued

nucleotide mutations are shown in red. (**B**) Analysis of HA-His3p abundance in *dds* mutant strains. Protein extraction and immunoblotting were performed as in ***Figure 4D***, using untagged BY4741 as a negative specificity control for the HA antibody. Strains indicated in red contain mutations in the HA-His3p +tail reporter gene. Strains that were subjected to whole-genome sequencing are indicated in blue and gray, with blue indicating those that contain a mutation in *DUH1* and gray indicating those that do not. (**C**) Table of *trans*-acting mutations identified by whole-genome sequencing. Strains containing *DUH1* mutations are listed in order of increasing total number of mutations. (**D**) Representative example of Sanger sequencing confirmation of *DUH1* mutations. Shown are sequencing traces across a region of *DUH1* for the parental selection strain and two *dds* mutants. Each *dds* mutant contains a nucleotide substitution (highlighted in yellow), compared to both the reference sequence and parental selection strain, corresponding to the mutation identified by whole-genome sequencing.

DOI: 10.7554/eLife.20069.011

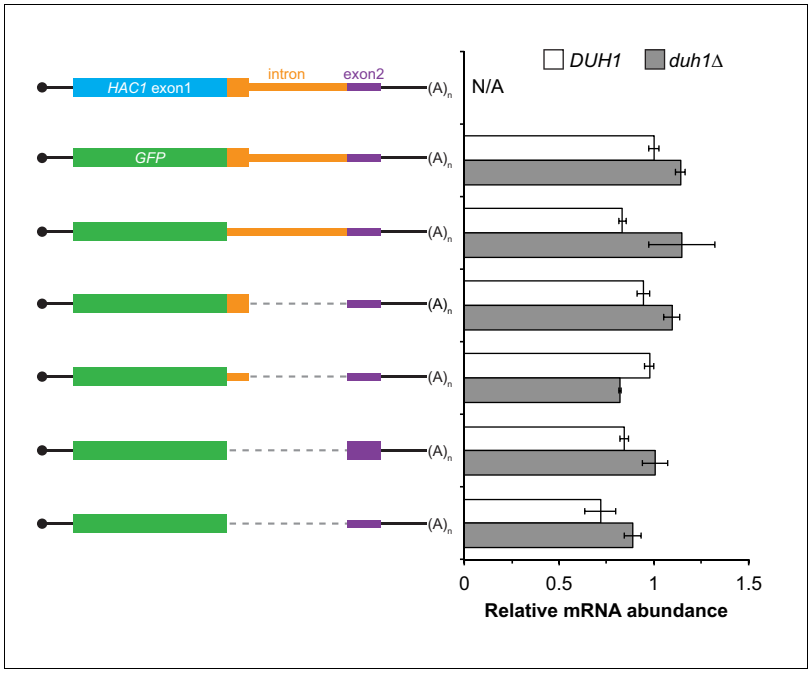

Figure 4—figure supplement 2. Additional analysis of *GFP* reporter constructs. RNA abundance measurements for *GFP* reporter mRNAs in the indicated strain backgrounds, analyzed as in ***Figure 2—figure supplement 1A*** using the same cultures as for flow cytometry analyses in ***Figure 4E***.
DOI: 10.7554/eLife.20069.012

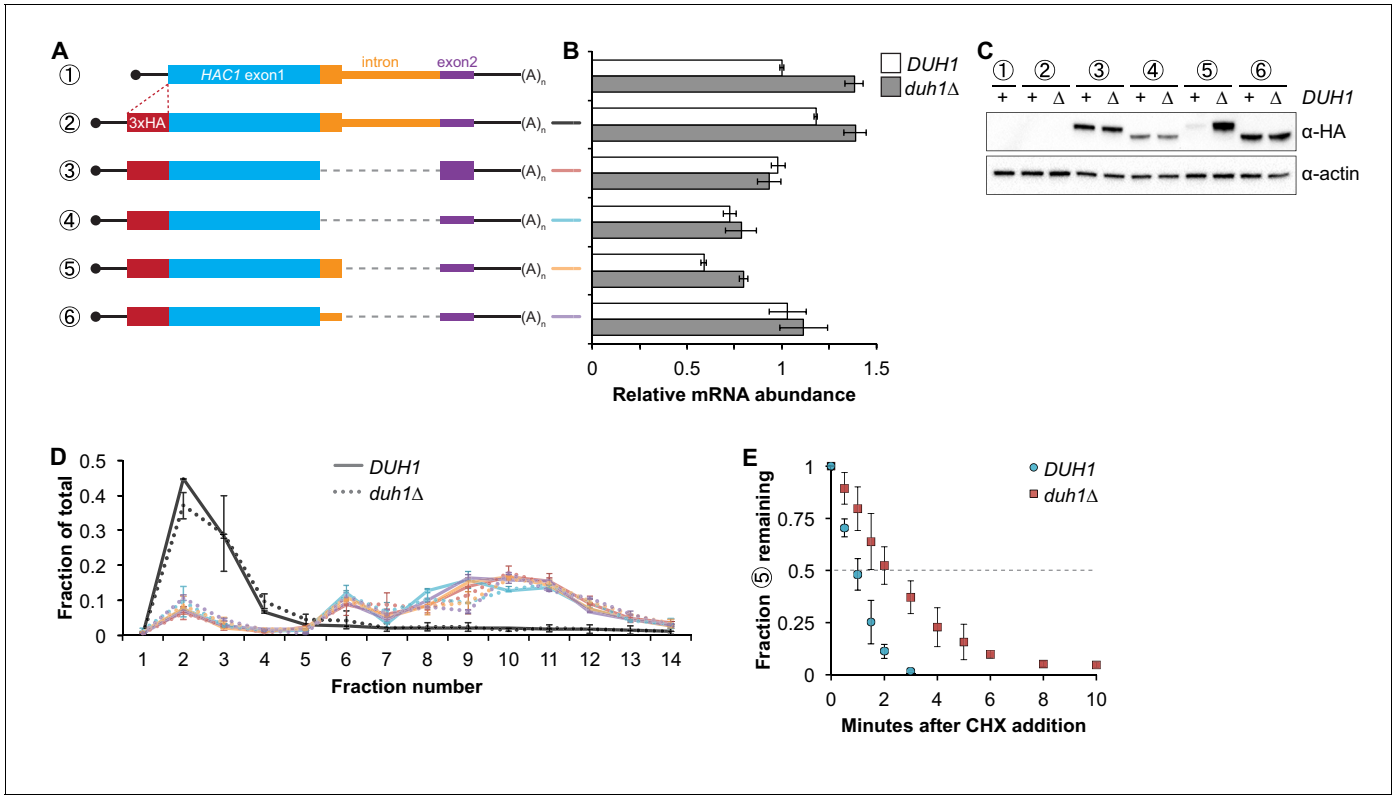

Figure 5. Effects of *DUH1* on expression and stability of Hac1p. (**A**) Design of 3xHA-tagged *HAC1* mRNA variants. Constructs are depicted as in ***Figure 2B***, with the location of the N-terminal 3xHA tag indicated. (**B**) RNA abundance measurements for *HAC1* mRNA variants. Total RNA was extracted from strains expressing the indicated mRNAs in either a *DUH1* or *duh1Δ* background. qRT-PCR was used to measure the abundances of *HAC1* variants relative to *ACT1* mRNA, with all data normalized to the abundance of construct 1 in strain BY4741. Shown are the mean ± SD (n = 2). (**C**) Effect of *DUH1* disruption on protein abundances. Strains expressing the indicated mRNAs depicted in (**A**) in either a *DUH1* or *duh1Δ* background were grown to mid-log phase. Extracts were prepared and immunoblotted for 3xHA-Hac1p and actin loading control. (**D**) Polysome analysis of 3xHA-tagged *HAC1* mRNA variants. Extracts were prepared in heparin-containing lysis buffer from strains expressing the mRNAs indicated in (**A**) in either a *DUH1* or *duh1Δ* background. Polysome analysis was performed as in ***Figure 1A***. (**E**) Analysis of protein degradation kinetics. Strains expressing construct 5 (depicted in **A**) in either a *DUH1* or *duh1Δ* background were grown to mid-log phase before being treated with cycloheximide (CHX) to halt translation. At the indicated time points, aliquots of cells were quenched in dry-ice-cold methanol and harvested by centrifugation. Protein extraction and immunoblotting were performed as in (**C**), except that a high-sensitivity antibody was used to detect 3xHA-Hac1^{u}p. Shown are the mean ± SD (n = 3), expressed as a fraction of protein detected at t = 0.

DOI: 10.7554/eLife.20069.013

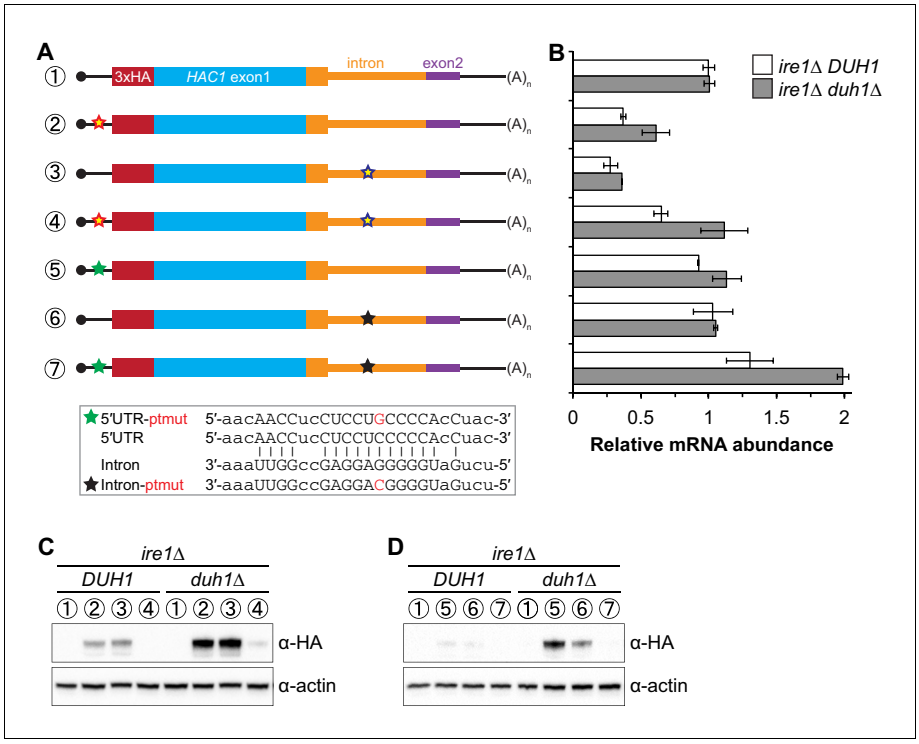

Figure 6. Relationship between base pairing– and degron-dependent repression. (**A**) Design of 3xHA-tagged *HAC1* mRNA variants. Constructs are depicted as in ***Figure 2B***. Colored stars indicate mutations to the base-pairing region, with specific nucleotide changes shown in ***Figure 2B*** (red and blue stars) or below (green and black stars) in red. (**B**) RNA abundance measurements for *HAC1* mRNA variants in the indicated strain backgrounds, analyzed as in ***Figure 5B***. (**C–D**) Effect of *DUH1* disruption on protein abundances. *ire1Δ* strains expressing the indicated mRNAs depicted in (**A**) in either a *DUH1* or *duh1Δ* background were analyzed as in ***Figure 5C***, except that a high-sensitivity antibody was used to detect 3xHA-Hac1^{u}p.

DOI: 10.7554/eLife.20069.014

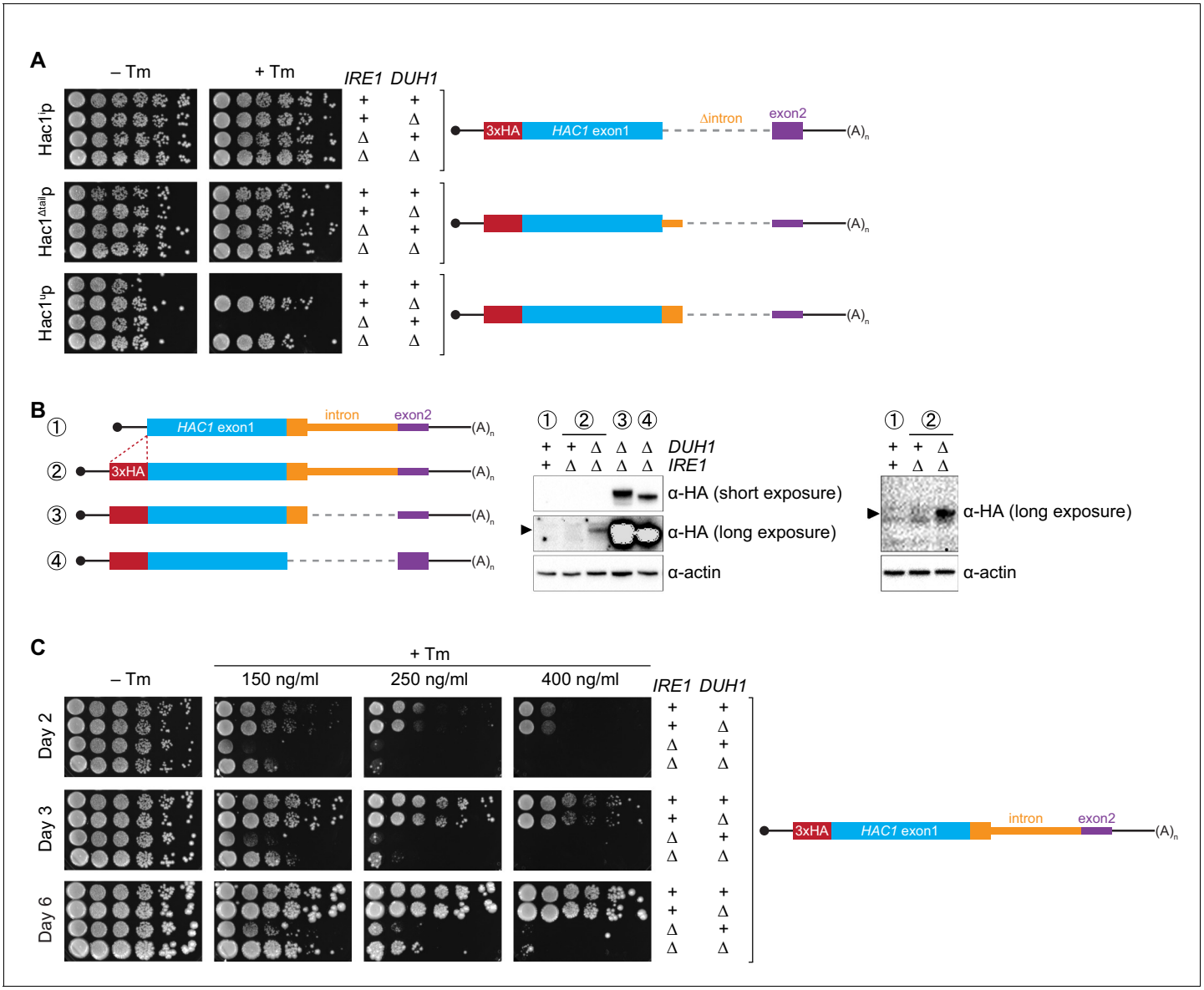

Figure 7. Requirement for *DUH1* to suppress Ire1p-independent activation of the UPR. (**A**) Analysis of Hac1p activity in the UPR. Strains expressing the indicated *HAC1* mRNA variants, with (+) or without (Δ) *IRE1* and/or *DUH1* present, were grown to saturation. 10-fold dilution series were plated on YPD without (–Tm) or with (+Tm) 400 ng/ml tunicamycin to induce ER stress. (**B**) Impact of *DUH1* on detection of Hac1^{u}p. Strains expressing the indicated mRNAs, with (+) or without (Δ) *IRE1* and/or *DUH1* present, were analyzed as in ***Figure 6C***. Black arrow indicates the position of Hac1^{u}p, which migrates more slowly than Hac1^{i}p. Construct 1, which lacks a 3xHA tag, was used as a negative control for anti-HA immunoblotting. (**C**) Effect of Duh1p-dependent degradation on the UPR. Strains expressing wild-type *HAC1* with an N-terminal 3xHA tag, with (+) or without (Δ) *IRE1* and/or *DUH1* present, were grown to saturation. 10-fold dilution series were plated on YPD without tunimacyin (–Tm) or containing the indicated concentration of tunicamycin (+Tm). Plates were imaged at days 2 (top), 3 (middle), and 6 (bottom).

DOI: 10.7554/eLife.20069.015

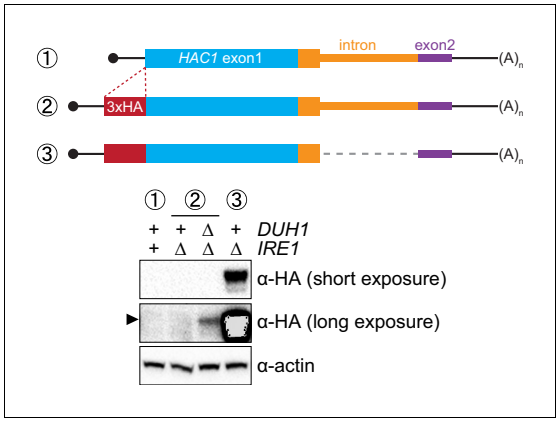

Figure 7—figure supplement 1. Ire1p-independent accumulation of Hac1p. Strains expressing the indicated mRNAs, with (+) or without (Δ) *IRE1* and/or *DUH1* present, were analyzed and presented as in ***Figure 7B***.

DOI: 10.7554/eLife.20069.016

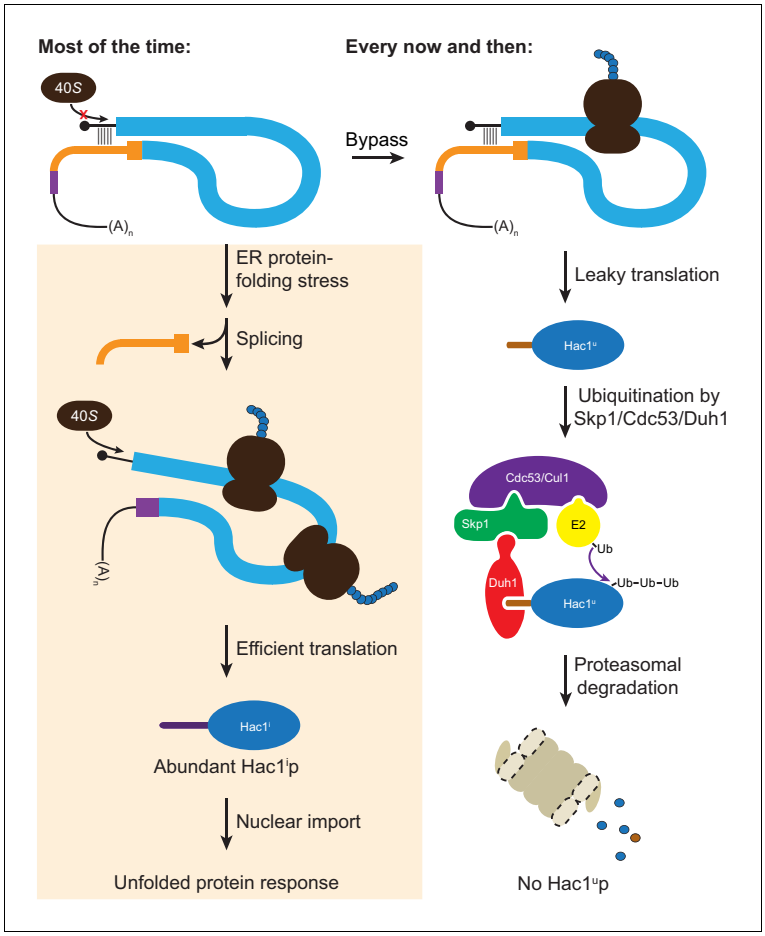

Figure 8. Fail-safe post-transcriptional silencing of unspliced *HAC1* mRNA. See the main text for a description.
DOI: 10.7554/eLife.20069.017